PHYSICAL REVIEW A **83**, 033423 (2011)

Direct observation of field-free alignment of asymmetric molecules in excited states

Chaochao Qin, Yuzhu Liu, Song Zhang, Yanmei Wang, Ying Tang, and Bing Zhang[*]
State Key Laboratory of Magnetic Resonance and Atomic and Molecular Physics, Wuhan Institute of Physics and Mathematics, Chinese Academy of Sciences, Wuhan, Hubei 430071, People's Republic of China and Graduate School of the Chinese Academy of Sciences, Beijing 100049, People's Republic of China

(Received 21 January 2011; published 31 March 2011)

The excited state dynamics of *o*-dichlorobenzene has been studied by femtosecond time-resolved photoelectron imaging. The lifetime of the first excited state S_1 of *o*-dichlorobenzene was determined to be 482 ± 10 ps. Field-free nonadiabatic alignment of the *o*-dichlorobenzene on the first excited state S_1 (with an asymmetry parameter $k = 0.153$) by a femtosecond laser pulse was observed via time-resolved photoelectron angular distributions. Rotational wave packet revivals on the S_1 state of the typical asymmetric molecule *o*-dichlorobenzene at 296 ps has been measured.

DOI: 10.1103/PhysRevA.83.033423 PACS number(s): 37.10.Vz, 33.80.−b, 33.80.Rv, 33.80.Eh

I. INTRODUCTION

Laser alignment—the application of moderately intense laser pulses to align neutral molecules along the polarization axis of a laser electric field—has grown over the past decade into an active research area with a broad variety of demonstrated and projected applications in areas such as ultrafast optics [1], x-ray absorption and diffraction [2,3], ultrafast imaging [4,5], high-order harmonic generation [6,7], molecular dynamics [8,9], and solution chemistry [10]. Although most studies to date have focused on the case of isolated rigid linear molecules subject to linearly polarized fields, recent research has generalized the method to asymmetric tops [11,12], solvated molecules [13], and surface-adsorbed molecules [14], and to complex systems such as small proteins [15] and molecular assembly and to new control opportunities.

When the laser pulse duration is longer than the rotational period of molecules, the alignment is called adiabatic alignment. As the laser pulse duration is shorter than the molecular rotational period, the laser-molecule interaction gives the molecule a rapid "kick" and a coherent rotational wave packet is therefore created. After the laser is off, the evolution of the wave packet results in transient alignment. This alignment is called nonadiabatic alignment. Both of these two kinds of alignments can prepare macroscopic ensembles with highly aligned molecules. Iodobenzene [16] (with an asymmetry parameter $k = -0.965$), serving as a typical asymmetric molecule, has been studied. However, field-free alignment is also expected for molecules possessing an inertia tensor that is much more asymmetric than that of iodobenzene.

For a detailed study of time evolution of wave-packet dynamics, time-resolved photoelectron imaging (TRPEI) has proven to be a powerful technique [17–20]. The TRPEI translates into the photoionization differential cross section, energy resolved to within the probe bandwidth. It thus provides both the energy and the angular distribution of the photoelectrons as well as their correlation as a function of time. In particular, the sensitivity of the photoelectron angular distribution to the electronic symmetry translates into useful information regarding the discrimination and visualization of wave-packet dynamics.

It is known that o-dichlorobenzene belongs to the C_{2v} point group. The A, B, and C rotational constants of the ground state S_0 have been calculated to be 1.894, 1.421, and 0.812 GHz, respectively, at the Becke three-parameter Lee-Yang-Parr (hybrid functional) (B3LYP)/6-311+G** level. The A', B', and C' rotational constants of the first excited state S_1 were calculated to be 1.886, 1.432, and 0.814 GHz, respectively, using configuration interaction singles (CIS)/6-311+G**. The asymmetry parameters $k = (2B-A-C)/(A-C)$ were determined to be 0.126 and 0.153 ($k = 0$ corresponding to the most asymmetry case) for the S_0 (A_1) and S_1 (A_1) states, respectively, suggesting that *o*-dichlorobenzene is a typical asymmetric molecule. In this paper, we present the study of nonadiabatic alignment of *o*-dichlorobenzene on excited state. We focus primarily on the alignment that follows the pulse turn-off but observe also alignment several hundreds of picoseconds (ps) later, corresponding to rotational wave-packet revivals.

II. EXPERIMENT

The details of our femtosecond (fs) laser system have been described elsewhere [21]. Briefly, the seed beam was generated by a commercial Ti : sapphire oscillator pumped by a cw second harmonic of a neodymium-doped yttrium orthovanadate (Nd : YVO_4) laser, and then amplified by a neodymium-doped yttrium lithium fluoride (Nd : YLF) pumped regenerative amplifier to generate a 1-kHz pulse train centered at 800 nm (with a 30-nm bandwidth, 45-fs pulse width) with a maximum energy of 1 mJ/pulse. This light was split into two equal intensity beams, one of which was frequency tripled to 267 nm, generated in a 0.2-mm-thick beta barium borate (BBO) crystal by sum frequency mixing of the second harmonic and the fundamental, to produce the pump light. The other beam served as the probe light. The probe beam was temporally delayed relative to the pump beam by a computer-controlled linear translation stage (PI, M-L01.4A1). The two laser beams were introduced into the vacuum chamber collinearly with a dichroic mirror, and focused with fused silica lenses of $f = 500$ and 350 mm, respectively. The polarizations of both beams were parallel to the detector plane. During

---

[*] Corresponding author: bzhang@wipm.ac.cn

1050-2947/2011/83(3)/033423(4)

experiments, typical pulse energies were ~3 μJ/pulse for the pump and ~60 μJ/pulse for the probe pulse.

The velocity map imaging setup [22] is similar to that designed by Eppink and Parker [23]. It consists of a molecular-beam source chamber and an ionization-flight detection chamber. The detection chamber was kept below 5×10^{-5} Pa with the molecular beam on. *o*-dichlorobenzene (99.9% purity) seeded in He was expanded into the source chamber with a stagnation pressure of 2 atm through a pulsed nozzle (General Valve, with a 0.5-mm orifice) with a repetition rate of 10 Hz. The supersonic molecular beam is collimated by a conical skimmer and intersects perpendicularly with the two laser beams in a two-stage ion lens region. Photoelectrons are extracted into a 36-cm field-free region, which is doubly shielded against stray magnetic fields by a μ-metal tube. At the end of the time-of-flight tube, the electrons strike a two-stage microchannel plate detector backed by a phosphor screen. The images on the screen are captured with a thermoelectrically cooled charge-coupled-device video camera (LAVISION Inc., Imager Intense). Each photoelectron image is the integration of more than 10 000 laser shots. The emission from the phosphor screen is monitored by a photomultiplier connected to a 1-GS/s digital phosphor oscilloscope (Tektronix Inc., TDS2012B) USB interfaced with a computer. A basis-set expansion (BASEX) transform [24] is applied to calculate the slices through the three-dimensional (3D) scattering distributions of the photoelectrons from the observed two-dimensional (2D) projection images.

III. RESULTS AND DISCUSSION

The band origin of the first excited S_1 state of *o*-dichlorobenzene is estimated to be at 4.49 eV from the resonance-enhanced multiphoton ionization [25]. In our experiment, *o*-dichlorobenzene was pumped to the first excited state S_1 by one-photon absorption at 267 nm, and then photoionized by further absorption of 800-nm photons. For typical time-of-flight mass spectra, three peaks are observed corresponding to the $C_6H_4Cl_2^+$ parent, $C_6H_4Cl^+$, and $C_6H_4^+$ ions, and the area ratio of $C_6H_4Cl_2{}^+$, $C_6H_4Cl^+$, and $C_6H_4^+$ is 12 : 1 : 1. By checking the ion intensities as a function of the delay time, we found the time profiles of $C_6H_4Cl^+$ and $C_6H_4^+$ ions have similar decay trends as the $C_6H_4Cl_2{}^+$ parent ion, so we believe that $C_6H_4Cl^+$ and $C_6H_4^+$ ions are from the dissociation of $C_6H_4Cl_2{}^+$ parent ions and have no contribution to the total photoelectron signal.

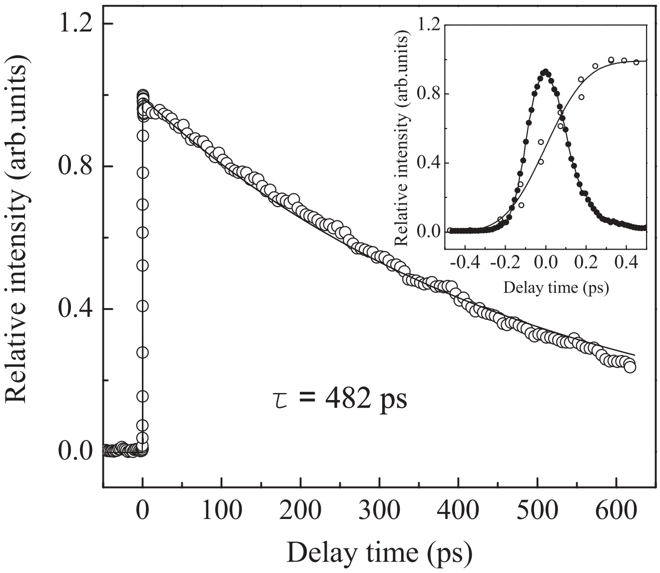

FIG. 1. Typical transient profile obtained by monitoring the *o*-dichlorobenzene parent-ion mass (147 amu) signal. The open circles are experimental data, and the solid line is the best fit to an exponential decay convoluted with a Gaussian response function of 260 fs. The inset (solid circles) is the cross-correlation curve of pump and probe pulses.

Figure 1 shows a typical transient profile obtained by monitoring the parent-ion intensity as a function of pump-probe delay time. The signal rises instantaneously after the pump pulse and then decays slowly in hundreds of picoseconds. The transient can be fit to an exponential decay of 482 ps convoluted with a Gaussian instrument response function of 260 fs. Previous spectroscopic studies [26] have reported that the fluorescence lifetime of the *o*-dichlorobenzene was estimated to be 1.4 ns for the band origin of S_1. Accordingly, the lifetime 482 ± 10 ps reflects the decay of the vibronic excited S_1 state of this molecule pumped at 267 nm. Possible deexcitation mechanisms are suggested that the initially excited S_1 state is predissociative via the repulsive triplet state, which is in consistent with that on the basis of the laser-induced fluorescence (LIF) experiment [26] and previous investigations on *p*-dichlorobenzene [27].

The photoelectrons generated by pump-probe photoionization are projected onto a 2D position-sensitive detector. Photoelectron images are acquired at different pump-probe time delays. In our experimental configuration with the linear and parallel polarization of the pump and probe laser beams, the

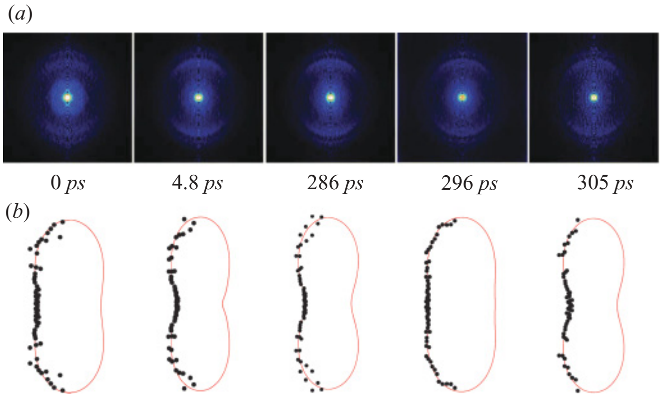

FIG. 2. (Color online) Time-resolved photoelectron images, photoelectron-angular distributions, in a $(1+4')$ resonance-enhanced multiphoton ionization via the S_1. The pump-laser wavelength was fixed to a $S_1 \leftarrow S_0$ transition (267 nm), and the probe-laser wavelength was 800 nm. The linear polarizations of the pump and probe lasers are aligned vertical in the plane of the figure. (a) BASEX transforms of the time-resolved photoelectron images corresponding to the slices through the 3D photoelectron velocity distributions at specified time delays. (b) Polar plots of the photoelectron-angular distributions corresponding to the second band associated with ionization from the S_1 to the D_1 at specified time delays. Solid lines are theoretical fits.

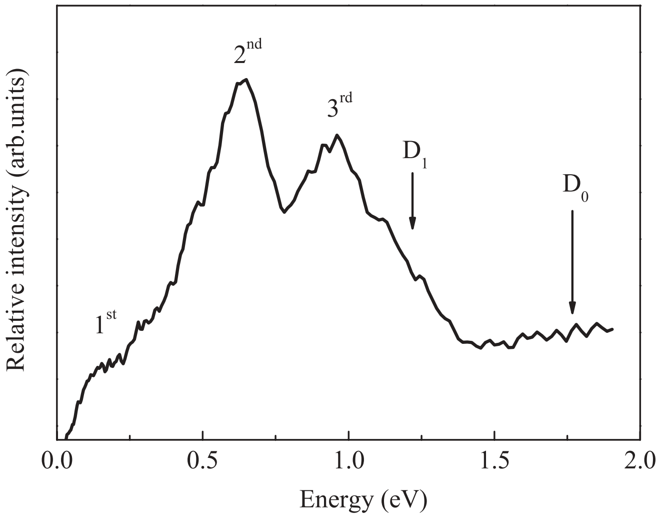

FIG. 3. Photoelectron kinetic energy distributions extracted from the images of Fig. 2. The arrows indicate the photoelectron energy (1.77 and 1.21 eV) expected for ionization to the zero vibrational level of the cation indicated by D_0 and D_1, by four-photon absorption of the probe pulse.

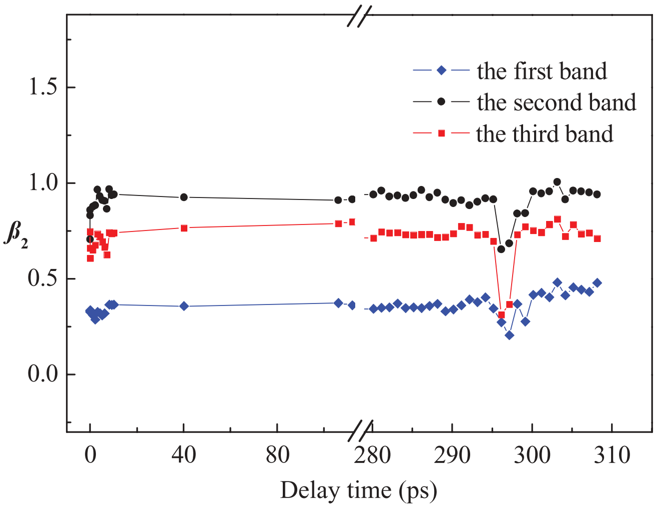

FIG. 5. (Color online) Anisotropy parameters of the first, second, and third bands as a function of pump-probe time delay.

laboratory frame photoelectron angular distributions (PADs) resulting from ionization can be expanded as [28]

$$I(\theta;t) = \sigma(t)[1+\beta_2(t)P_2(\cos\theta)+\beta_4(t)P_4(\cos\theta) + \beta_6(t)P_6(\cos\theta)+\beta_8(t)P_8(\cos\theta) + \beta_{10}(t)P_{10}(\cos\theta)], \qquad (1)$$

where $\sigma(t)$ is the integral cross section, $\beta_L(t)$ are the anisotropy parameters, $P_L(\cos\theta)$ are Legendre polynomials, and θ is the angle between the laser polarization direction and the electron recoil direction. We found from β_4 to β_{10} to be negligible. Figure 2(a) shows a series of photoelectron images measured at different pump-probe time delays, and the polarization of the pump and probe lasers are both vertical in the figure. The images are inverted by the BASEX method [24], representing a section of the 3D photoelectron scattering distribution. Three well-resolved concentric bands are observed with different radii corresponding to photoelectron kinetic energies (PKE) of 0.15, 0.65, and 0.96 eV, which are assigned as the first, second, and the third bands in the order of increasing energy. The corresponding photoelectron kinetic energy distributions of these images are shown in Fig. 3. The arrows indicate the photoelectron kinetic energy (1.77 and 1.21 eV) that are expected for ionization to the zero vibrational level of the cation indicated by D_0 and D_1, by four-photon absorption of probe pulse. The PADs at individual PKEs can be extracted from the observed images. Figure 2(b) shows the polar plots of PAD observed for the second band at corresponding time delays as Fig. 2(a), and it is obvious that the PAD revives at 296 ps.

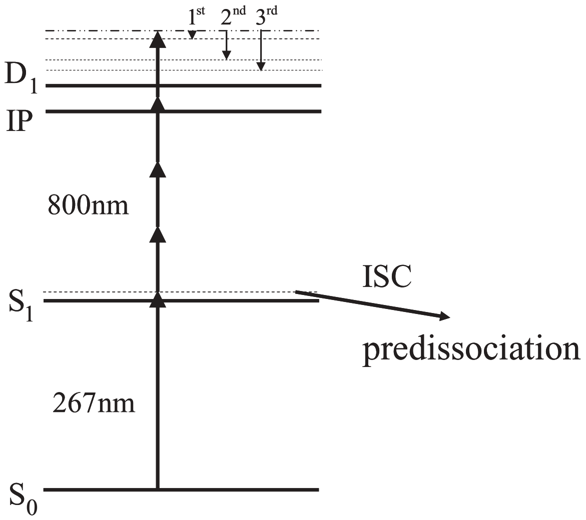

FIG. 4. A schematic illustration of the possible ionization pathways. Here, 1st (Apply superscript formatting to st.) 2nd, and 3rd (Apply superscript formatting to rd.) correspond to the first, second, and third bands.

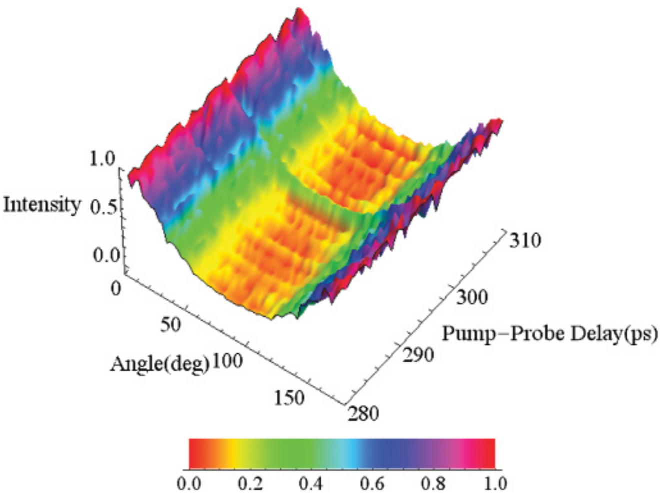

FIG. 6. (Color online) Time dependence of photoelectron angular distribution obtained for PEI via S_1. Pump-probe delay was scanned from 280 to 310 ps with a 1-ps interval. The first full revival of the rotational wave packet is at 296 ps.

The ionization energy (IE) of *o*-dichlorobenzene is determined to be 73237 cm^{-1} (9.08 eV) via mass analyzed threshold ionization (MATI) spectroscopy [25] and photoelectron spectroscopy (PES) [29]. The initially excited S_1 state can be ionized by absorbing three probe photons at 800 nm, reaching a total energy of ~9.30 eV which is just ~0.22 eV above the *o*-dichlorobenzene adiabatic IE. It is known that the pump laser (267 nm) mainly populates the breathing vibration mode in the S_1 state, and there is no peak near the band origin (0^+) of the cationic ground state D_0 of *o*-dichlorobenzene when the breathing mode in the S_1 state as the intermediate state in the MATI spectra [30], which demonstrates that the Franck-Condon overlaps between the breathing vibration mode in S_1 and 0^+ of the D_0 are poor. Therefore, the assignments of the three bands are probably all associated with the $(1 + 4')$ process. A schematic illustration of the possible ionization pathways is shown in Fig. 4.

Figure 5 shows the β_2 coefficients of the first, second, and third band extracted from a series of the photoelectron images, respectively, which are acquired at the same condition except different delay time. At the delay time of 0 and 296 ps, the remarkable decrease of the β_2 coefficient is observed, which indicates the wave-packet revivals and field-free molecular axis alignment.

Figure 6 shows the time dependence of the PADs following ionization of the S_1 state. Photoelectron images were recorded at pump-probe delay intervals of 1 ps around the positions of the full revival of the rotational wave packet at 296 ps. At the full revival, the PADs exhibits a small enhancement near the direction of $\theta = 90^\circ$. In the present case, the pump pulse creates a time-dependent molecular axis alignment in the S_1 state; since the S_1 states are ionized instantaneously within a probe laser pulse, the PAD is modulated only by the time dependence of molecular axis alignment in the S_1 state.

As mentioned above, we have observed field-free nonadiabatic alignment of a much more asymmetric molecule with an asymmetry parameter $k = 0.153$.

IV. CONCLUSIONS

We have used femtosecond time-resolved pump-probe photoelectron imaging to observe ultrafast processes arising from the optically excited states of *o*-dichlorobenzene in real time. The lifetime of the first excited state S_1 of *o*-dichlorobenzene was determined to be ~482 ± 10 ps. Field-free alignment of *o*-dichlorobenzene on an excited state by a femtosecond laser pulse was observed though time evolution of the anisotropy parameters. Rotational wave-packet revivals on S_1 excited electronic states of *o*-dichlorobenzene as long as 296 ps were observed via time-resolved photoelectron angular distribution.

ACKNOWLEDGMENTS

This work was supported by the National Natural Science Foundation of China under Grants No. 10704083, No. 20973194, and No. 20903116, and the Innovation Foundation of Chinese Academy of Sciences under Grant No. KJCX1-YW-N30.

[1] R. A. Bartels, T. C. Weinacht, N. Wagner, M. Baertschy, C. H. Greene, M. M. Murnane, and H. C. Kapteyn, Phys. Rev. Lett. **88**, 013903 (2001).

[2] J. C. H. Spence, K. Schmidt, J. S. Wu, G. Hembree, U. Weierstall, B. Doak, and P. Fromme, Acta Crystallogr., Sect. A: Found.Crystallogr. **61**, 237 (2005).

[3] E. R. Peterson *et al.*, Appl. Phys. Lett. **92**, 094106 (2008).

[4] J. Itatani, J. Levesque, D. Zeidler, H. Niikura, H. Pepin, J. C. Kieffer, P. B. Corkum, and D. M. Villeneuve, Nature (London) **432**, 867 (2004).

[5] M. Meckel *et al.*, Science **320**, 1478 (2008).

[6] T. Kanai, S. Minemoto, and H. Sakai, Nature (London) **435**, 470 (2005).

[7] C. Vozzi *et al.*, Phys. Rev. Lett. **95**, 153902 (2005).

[8] S. S. Viftrup, V. Kumarappan, L. Holmegaard, C. Z. Bisgaard, H. Stapelfeldt, M. Artamonov, E. Hamilton, and T. Seideman, Phys. Rev. A **79**, 023404 (2009).

[9] Y. Mairesse *et al.*, New J. Phys. **10**, 25028 (2008).

[10] S. Ramakrishna and T. Seideman, Phys. Rev. Lett. **99**, 103001 (2007).

[11] M. D. Poulsen, E. Peronne, H. Stapelfeldt, C. Z. Bisgaard, S. S. Viftrup, E. Hamilton, and T. Seideman, J. Chem. Phys. **121**, 783 (2004).

[12] K. F. Lee, D. M. Villeneuve, P. B. Corkum, A. Stolow, and J. G. Underwood, Phys. Rev. Lett. **97**, 173001 (2006).

[13] S. Ramakrishna, and T. Seideman, Phys. Rev. Lett. **95**, 113001 (2005).

[14] M. G. Reuter, M. Sukharev, and T. Seideman, Phys. Rev. Lett. **101**, 208303 (2008).

[15] J. C. H. Spence and R. B. Doak, Phys. Rev. Lett. **92**, 198102 (2004).

[16] E. Peronne, M. D. Poulsen, C. Z. Bisgaard, H. Stapelfeldt, and T. Seideman, Phys. Rev. Lett. **91**, 043003 (2003).

[17] Toshinori Suzuki, Annu. Rev. Phys. Chem. **57**, 555 (2006).

[18] M. Tsubouchi, B. J. Whitaker, L. Wang, H. Kohguchi, and T. Suzuki, Phys. Rev. Lett. **86**, 4500 (2001).

[19] T. Seideman, Annu. Rev. Phys. Chem. **53**, 41 (2002).

[20] A. Stolow, A. E. Bragg, and D. M. Neumark, Chem. Rev. **104**, 1719 (2004).

[21] Z. Wei, F. Zhang, Y. Wang and B. Zhang, Chin. J. Chem. Phys. **20**, 419 (2007).

[22] Z. Z. Cao, Z. R. Wei, L. Q. Hua, C. J. Hu, S. Zhang, and B. Zhang, J. Chem. Phys. **130**, 144309 (2009).

[23] A. T. J. B. Eppink and D. H. Parker, Rev. Sci. Instrum. **68**, 3477 (1997).

[24] V. Dribinski, A. Ossadtchi, V. A. Mandelshtam, and H. Reisler, Rev. Sci. Instrum. **73**, 2634 (2002).

[25] A. Gaber, M. Riese, and J. Grotemeyer, J. Phys. Chem. A **112**, 425 (2008).

[26] A. Shimoda, T. Hikida, and Y. Mori, J. Chem. Phys. **83**, 1309 (1979).

[27] L. W. Yuan, J. Y. Zhu, Y. Q. Wang, L. Wang, J. L. Bai, and G. Z. He, Chem. Phys. Lett. **410**, 352 (2005).

[28] C. N. Yang, Phys. Rev. **74**, 764 (1948).

[29] B. Ruscic, L. Klasinc, A. Wolf, and J. V. Knop, J. Phys. Chem. **85**, 1486 (1981).

[30] A. Gaber, M. Riese, and J. Grotemeyer, Phys. Chem. Chem. Phys. **10**, 1168 (2008).